

Geographical isolation versus dispersal: Relictual alpine grasshoppers support a model of interglacial diversification with limited hybridization

Joaquín Ortego¹  | L. Lacey Knowles² 

¹Department of Integrative Ecology, Estación Biológica de Doñana (EBD-CSIC), Seville, Spain

²Department of Ecology and Evolutionary Biology, University of Michigan, Ann Arbor, Michigan, USA

Correspondence

Joaquín Ortego, Estación Biológica de Doñana, EBD-CSIC, Avda. Américo Vespucio 26, E-41092 Seville, Spain.
Email: joaquin.ortego@csic.es

Funding information

Spanish Ministry of Economy, Industry and Competitiveness, Grant/Award Number: CGL2014-54671-P and CGL2017-83433-P; European Social Fund, Grant/Award Number: CGL2014-54671-P and CGL2017-83433-P

Abstract

Alpine biotas are paradigmatic of the countervailing roles of geographical isolation and dispersal during diversification. In temperate regions, repeated distributional shifts driven by Pleistocene climatic oscillations produced both recurrent pulses of population fragmentation and opportunities for gene flow during range expansions. Here, we test whether a model of divergence in isolation vs. with gene flow is more likely in the diversification of flightless alpine grasshoppers of the genus *Podisma* from the Iberian Peninsula. The answer to this question can also provide key insights about the pace of evolution. Specifically, if the data fit a divergence in isolation model, this suggests rapid evolution of reproductive isolation. Genomic data confirm a Pleistocene origin of the species complex, and multiple analytical approaches revealed limited asymmetric historical hybridization between two taxa. Genomic-based demographic reconstructions, spatial patterns of genetic structure and range shifts inferred from palaeodistribution modelling suggest severe range contraction accompanied by declines in effective population sizes during interglacials (i.e., contemporary populations confined to sky islands are relicts) and expansions during the coldest stages of the Pleistocene in each taxon. Although limited hybridization during secondary contact leads to phylogenetic uncertainty if gene flow is not accommodated when estimating evolutionary relationships, all species exhibit strong genetic cohesiveness. Our study lends support to the notion that the accumulation of incipient differences during periods of isolation were sufficient to lead to lineage persistence, but also that the demographic changes, dispersal constraints and spatial distribution of the sky islands themselves mediated species diversification in temperate alpine biotas.

KEYWORDS

distributional shifts, genetic cohesiveness, hybridization, introgression, Pleistocene, reticulate evolution, speciation

This is an open access article under the terms of the Creative Commons Attribution License, which permits use, distribution and reproduction in any medium, provided the original work is properly cited.

© 2021 The Authors. *Molecular Ecology* published by John Wiley & Sons Ltd.

1 | INTRODUCTION

The opportunities for divergence in isolation, but also the counteracting effects of gene flow during periods of secondary contact, are quintessential processes of Pleistocene speciation in alpine and montane biotas from temperate regions (Hewitt, 2000). Isolation of populations in glacial (Carstens & Knowles, 2007) or interglacial (Bennett & Provan, 2008) refugia during the climatic oscillations of the Pleistocene is likely to have exposed them to different selective regimes and increased genetic drift, which ultimately are hypothesized to have promoted divergence and speciation (Hewitt, 1996; Stewart et al., 2010). Conversely, latitudinal displacements to or from glacial refugia and downslope movements towards lower elevation areas during ice ages may contribute to geographical contact of gene pools that had remained isolated over extended periods of time (Knowles & Massatti, 2017; Maier et al., 2019; Tonzo & Ortego, 2021). If incipient speciation during geographical isolation is not accompanied by effective reproductive isolation, secondary contact will lead to post-divergence gene flow (Hewitt, 2000). Depending on the permeability to gene exchange between previously allopatric lineages, the consequences of such process will range from speciation reversal (e.g., Maier et al., 2019) to different levels of introgressive hybridization (e.g., Melo-Ferreira et al., 2005). For these reasons, Pleistocene glacial–interglacial cycles are hypothesized to have acted both as “species pumps” and as “melting pots,” creating opportunity for divergence and gene exchange across different stages along the continuum of speciation (April et al., 2013; Ebdon et al., 2021; Haffer, 1969; Hewitt, 1996, 2000; Knowles, 2001; Petit et al., 2003). Climate oscillations during the Quaternary are thus expected to have promoted reticulate speciation in many organism groups, rather than a strictly bifurcating evolutionary history of species divergence (Nevado et al., 2018; Thom et al., 2018).

An accurate reconstruction of the history of species divergence is a prerequisite for inferring the tempo and mode of speciation and testing alternative biogeographical and macro-evolutionary hypotheses regarding the processes underlying observed patterns of biological diversity (Nylander et al., 2008; Rangel et al., 2015; Tariel et al., 2016). However, the phylogenetic relationships of recently diverged species can be obscured by unresolved nodes (i.e., polytomies) (e.g., Kutschera et al., 2014; Takahashi et al., 2014). Phylogenetic uncertainties are frequently a consequence of incomplete lineage sorting (ILS) of ancestral polymorphism (Maddison & Knowles, 2006) and/or deviations from strictly bifurcating lineages due to horizontal gene transfer, hybrid speciation or introgression (Mallet et al., 2016; McBreen & Lockhart, 2006). Identifying the causes of phylogenetic conflict (i.e., reticulation vs. ILS) is essential for distinguishing among alternative evolutionary pathways (e.g., de Manuel et al., 2016; Schrago & Seuanez, 2019; Thom et al., 2018), which can ultimately provide key insights about the pace of speciation (Rosindell et al., 2010; Sukumaran & Knowles, 2017). However, this task is more daunting in recent Pleistocene radiations in which species may have weak reproductive barriers and short interspeciation times that

often co-occur with secondary introgression (i.e., post-divergence gene flow) (Nevado et al., 2018; Wen et al., 2016). In the last decade, increased capacity to generate large genomic data sets in nonmodel organisms has been critical to overcoming statistical uncertainties contributed by limited genetic information. This has also driven the development of numerous analytical approaches aimed at resolving gene tree discordances and detecting admixture (reviewed in Payseur & Rieseberg, 2016). Thanks to these analytical advances, we can now test speciation hypotheses that depart from models of divergence in strict isolation, which is key to considering whether introgressive hybridization is a component of the evolutionary portrait of diversification (e.g., de Manuel et al., 2016; Thom et al., 2018). However, given the assumptions and limitations inherent to each available approach, corroboration across multiple lines of evidence for complex histories of diversification is recommended (for details, see Payseur & Rieseberg, 2016).

Here, we use genomic data to evaluate the countervailing effects of dispersal and isolation on the speciation process and determine whether population isolation driven by Pleistocene glacial cycles triggered the necessary mechanisms for long-lasting genetic cohesion of lineages or if, on the contrary, extensive gene flow during periods of secondary contact have impaired their persistence and the formation of new species (Dynesius & Jansson, 2014). Specifically, we apply an integration of multiple approaches to unravel a Pleistocene diversification history of alpine grasshoppers of the genus *Podisma* from the Iberian Peninsula (Orthoptera: Acrididae) (Morales-Agacino, 1951). As the southernmost distributional limit of the genus, the region hosts three species distributed in allopatry across different mountain ranges (Cigliano et al., 2021; Figure 1). The three taxa are distributed at elevations >1200 m, restricted to montane and alpine open habitats dominated by low grasslands and dwarf shrub formations (e.g., *Juniperus* sp., *Vaccinium* sp. and *Rhododendron* sp.), which are interspersed with patches of bare ground and rocks (Presa et al., 2016a, 2016b; Zuna-Kratky et al., 2016). As such, their contemporary populations are extremely fragmented across sky islands of suitable habitat embedded in an inhospitable matrix characteristic of the Mediterranean climate (Cigliano et al., 2021; Presa et al., 2016a, 2016b; Zuna-Kratky et al., 2016). There are no clear phenological differences among the taxa; the three species are univoltine (i.e., a single generation per year) with adult populations peaking in July–August (Morales-Agacino, 1951; Zuna-Kratky et al., 2016; J. Ortego, personal observation). They are very similar in external appearance and are flightless, with *Podisma pedestris* and *P. carpetana* being micropterous and *P. cantabricae* apterous, although rare macropterous (i.e., fully winged) forms have occasionally been described in *P. pedestris* (Lemonnier-Darcemont & Darcemont, 2014; Morales-Agacino, 1951). Capture–mark–release–recapture studies on *P. pedestris* indicate that these taxa exhibit very low dispersal capacities and a marked philopatric behaviour (Barton & Hewitt, 1981, 1982; Mason et al., 1995). Due to this limited dispersal ability and strict habitat requirements, we hypothesize that recurrent pulses of population expansions and contractions during

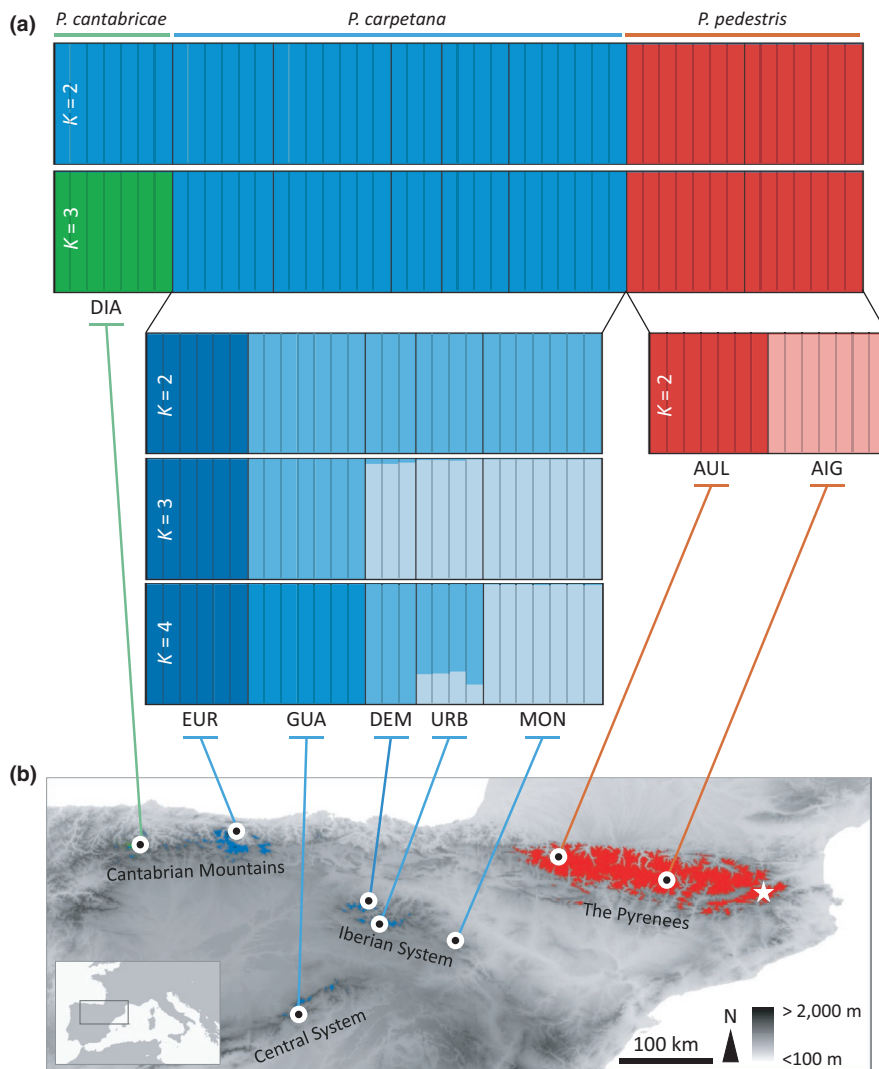


FIGURE 1 (a) Results of genetic assignments for *Podisma pedestris*, *P. carpetana* and *P. cantabricae* based on the Bayesian method implemented in the program STRUCTURE. Hierarchical STRUCTURE analyses were run for all species and independently for populations of *P. pedestris* and *P. carpetana*. Analyses are based on a random subset of 10,000 SNPs. Thin vertical lines separate individuals and thick lines demarcate sampling sites, with each individual partitioned into K coloured segments proportional to the individual's estimated ancestry proportions; population codes are described in Table S1. (b) Map showing sampling localities (black dots with white rings) across the northern half of the Iberian Peninsula (see map inset for focal area), main geographical features (mountain ranges) and the distribution of each taxon (red: *P. pedestris*; blue: *P. carpetana*; green: *P. cantabricae*) as predicted by species-specific environmental niche models (ENMs). A white star indicates the sampling locality for the outgroup *Cophopodisma pyrenaica*. Elevation shown by grey shading, with darker areas corresponding to higher elevations

Pleistocene glacial cycles have contributed to genetic isolation and speciation, but that the shifting distributions also generated repeated opportunities for post-divergence gene flow (e.g., Barton, 1980; Keller et al., 2008). To accommodate an evolutionary history that may depart from assumptions of divergence in isolation and to gain insights into the processes underlying speciation that includes the possibility of post-divergence gene flow, we integrate a comprehensive suite of phylogenomic and population genomic approaches with palaeoclimate-based reconstructions of species distributions. Specifically, we apply the multispecies coalescent (MSC) model to infer phylogenetic relationships among taxa and identify nodes with potential conflict that might be indicative of either ILS or reticulation. Then, we perform phylogenetic tests to distinguish ILS from introgression and use a model-based approach to evaluate alternative scenarios of post-divergence gene flow or lack thereof. Using environmental niche modelling and palaeoclimate-based reconstructions of species distributions, we infer range shifts during glacial/interglacial periods in each species and use this framework to determine which expectations in terms of population fragmentation and secondary contact are most probable given species divergence,

past demography and introgressive hybridization estimated based on the genomic data.

2 | MATERIALS AND METHODS

2.1 | Population sampling

Occurrence records from the literature were used to design sampling and guide collection of specimens from populations representative of the distribution range of each of the three *Podisma* taxa from the Iberian Peninsula: *Podisma pedestris* (Linnaeus, 1758), *Podisma carpetana* Bolívar, 1898, and *Podisma cantabricae* Morales-Agacino, 1950 (Figure 1; details given in Table S1). Seven specimens of *Cophopodisma pyrenaica* (Fischer, 1853) (tribe Podismini; Cigliano et al., 2021) were used as an outgroup in phylogenomic analyses and ABBA/BABA tests (Table S1). Spatial coordinates were recorded using a Global Positioning System (GPS) and whole specimens were preserved at -20°C in 1500 μl of 96% ethanol until needed for genomic analyses.

2.2 | Genomic library preparation and processing

We used NucleoSpin Tissue (Macherey-Nagel) kits to extract and purify DNA from a hind leg of each individual. We processed genomic DNA into one genomic library using the double-digestion restriction-site associated DNA sequencing procedure (ddRADseq) described in Peterson et al. (2012). In brief, we digested DNA with the restriction enzymes *MseI* and *EcoRI* (New England Biolabs) and ligated Illumina adaptors including unique 7-bp barcodes to the digested fragments of each individual. We pooled ligation products and size-selected 475–580 bp fragments with a Pippin Prep machine (Sage Science), amplified the fragments by PCR (polymerase chain reaction) with 12 cycles using the iProof High-Fidelity DNA Polymerase (Bio-Rad), and sequenced the library in a single-read 150-bp lane on an Illumina HiSeq2500 platform at The Centre for Applied Genomics (Toronto, ON, Canada). Raw sequences were demultiplexed and preprocessed using STACKS version 1.35 (Catchen et al., 2013) and assembled using PYRAD version 3.0.66 (Eaton, 2014); see Methods S1 for details on sequence assembling and data filtering. The choice of different filtering and assembling thresholds had a little impact on the obtained inferences (see Section 3; e.g., Eaton, 2014; Ortego et al., 2018). For this reason, unless otherwise indicated, all downstream analyses were performed using data sets of unlinked single nucleotide polymorphisms (SNPs) (i.e., using a single SNP per RAD locus) obtained with PYRAD considering a clustering threshold of sequence similarity of 0.85 ($W_{\text{clust}} = 0.85$) and excluding loci that were not present in at least 20 individuals ($\text{minCov} = 20$). We used the option *relatedness2* in VCFTOOLS to calculate the relatedness among all pairs of genotyped individuals and to exclude the possibility that we had sampled close relatives within each study population (Danecek et al., 2011; Manichaikul et al., 2010).

2.3 | Quantifying genetic structure

We analysed population genetic structure and admixture using the Bayesian Markov chain Monte Carlo (MCMC) clustering method implemented in the program STRUCTURE version 2.3.3 (Pritchard et al., 2000). We conducted STRUCTURE analyses hierarchically, initially analysing data from all populations and species jointly and, subsequently, running independent analyses for subsets of populations assigned to the same genetic cluster in the previous hierarchical-level analysis (Janes et al., 2017; Pritchard et al., 2000). We ran STRUCTURE using a random subset of 10,000 SNPs with 200,000 MCMC cycles after a burn-in step of 100,000 iterations, and assuming correlated allele frequencies and admixture (Pritchard et al., 2000). We performed 15 independent runs for each value of K genetic clusters, where K ranged from 1 to $n + 1$ for each data set of n populations, to estimate the most probable number of clusters. We retained the 10 runs with the highest likelihood for each K -value. As recommended by Gilbert et al. (2012) and Janes et al. (2017), we used two statistics to interpret the number of genetic clusters (K) that best describes our data: log probabilities of $\text{Pr}(X|K)$ (Pritchard et al., 2000) and ΔK (Evanno

et al., 2005). These statistics were calculated as implemented in STRUCTURE HARVESTER (Earl & vonHoldt, 2012). We used CLUMPP version 1.1.2 and the Greedy algorithm to align multiple runs of STRUCTURE for the same K -value (Jakobsson & Rosenberg, 2007) and DISTRUCT version 1.1 (Rosenberg, 2004) to visualize the individual's probabilities of genetic cluster membership as bar plots. Complementary to Bayesian clustering analyses, we performed principal component analyses (PCAs) as implemented in the R version 4.0.3 (R Core Team, 2021) package *adegenet* (Jombart, 2008). Before running the PCAs, we replaced missing data by the mean frequency of the corresponding allele estimated across all samples (Jombart, 2008).

2.4 | Phylogenomic inference

We estimated species trees using two coalescent-based methods: SNAPP version 1.3 (Bryant et al., 2012) as implemented in BEAST version 2.4.1 (Bouckaert et al., 2014) and SVDQUARTETS (Chifman & Kubatko, 2014) as implemented in PAUP* version 4.0a152 (Swofford, 2002).

2.4.1 | SNAPP

For the SNAPP analyses, we ran two independent replicates of >2 million generations sampled every 1000 steps (i.e., >2000 retained genealogies), removing 10% of trees as burn-in. Stationarity and convergence of the chains was assessed with TRACER version 1.4 to confirm that effective sample sizes (ESS) for all parameters were >200. We combined tree and log files for replicated runs using LOG-COMBINER version 2.4.1 and used TREEANNOTATOR version 1.8.3 to obtain maximum clade credibility trees and TREESETANALYSER version 2.4.1 to identify species trees that were contained in the 95% highest posterior density (HPD) set. Pilot analyses with different values of the shape (α) and inverse scale (β) parameters of the gamma prior distribution ($\alpha = 2, \beta = 200$; $\alpha = 2, \beta = 2000$; $\alpha = 2, \beta = 20,000$) for the population size parameter (θ), leaving default settings for all other parameters, yielded the same topology (not shown); only results for the intermediate prior for theta ($\alpha = 2, \beta = 2000$) are presented. The full set of trees was displayed with DENSITREE version 2.2.1 (Bouckaert, 2010), which is expected to show fuzziness in parts of the tree due to gene flow or other causes of phylogenetic conflict. Due to large computational demands of SNAPP, we only included three individuals per population for the ingroup.

2.4.2 | SVDQUARTETS

We ran SVDQUARTETS to estimate the evolutionary relationships of populations from each species (i.e., a population/species tree; Knowles & Carstens, 2007) by evaluating 10,000 random quartets from the data set; uncertainty in relationships was quantified using 100 bootstrapping replicates. Given the low computational burden of SVDQUARTETS in comparison with SNAPP, we analysed six SNP matrices obtained

by setting different values of clustering thresholds ($W_{\text{clust}} = 0.85$ and 0.90) and minimum taxon coverage for a locus ($\text{minCov} = 10, 20$ and 30) (see Methods S1). This allowed us to assess the impact of different proportions of missing data and number of loci on the estimated topology and patterns of branch support (Huang & Knowles, 2016; Nogueras et al., 2018; Takahashi et al., 2014).

2.5 | Analyses of introgression

Although phylogenetic analyses tended to support *P. carpetana* and *P. cantabricae* as sister taxa, the relationships among the three species often remained unresolved (see Section 3.3). To determine the role of ILS versus introgression in explaining such conflicting phylogenetic relationships, we tested the possibility of post-divergence gene flow using a comprehensive suite of approaches detailed below. Note that these analyses (with the exception of PHYLONETWORKS) were carried out sequentially using one representative population per species, and then testing all population combinations, because intraspecific population structure (see Figure 1) can confound analyses that assume panmixia within species.

2.5.1 | Phylogenetic networks

We used Species Networks applying Quartets (SNAQ) implemented in PHYLONETWORKS (Solís-Lemus et al., 2017) to determine whether a strictly bifurcating phylogenetic tree (i.e., no hybridization) or a phylogenetic network (i.e., one or more introgression events) better explains the evolutionary history of *Podisma* grasshoppers. SNAQ performs maximum pseudo-likelihood estimation of phylogenetic networks using the multispecies coalescent model and quartet-based concordance analyses (Solís-Lemus et al., 2017) to infer the most likely network, depict the major phylogenetic topology ("major edge") and past introgression events ("minor edges"), and calculate γ , the vector of inheritance probabilities describing the proportion of genes inherited by a hybrid node from one of its parents (Solís-Lemus et al., 2017). The MAGNET version 0.1.5 pipeline (J. C. Bagley, <http://github.com/justincbagley/MAGNET>) was used to split each locus contained in the PYRAD output file ".gphocs" into a separate phylip-formatted alignment file and run RAXML version 8.2.12 (Stamatakis, 2014) to infer a maximum-likelihood (ML) gene tree for each locus with the GTR+GAMMA model and 100 bootstrap replicates. Prior to obtaining gene trees, we applied TRIMAL version 1.2 (Capella-Gutiérrez et al., 2009) to our phylip data set to filter out loci with a high mean percentage of identity (>0.95) across the multisequence alignment and retain only those (1447 loci) that are most informative (Bernardes et al., 2007). We used these gene trees and PHYLONETWORKS to estimate quartet concordance factors (CFs), defined as the proportion of genes that support each possible relationship between each set of four taxa. We used the topology obtained with SNAPP as a starting tree and estimated the best phylogenetic network testing a varying number of reticulation events (h from 0 to

5), each optimized with 10 independent runs. The optimal number of reticulation events was chosen using a heuristic approach by plotting negative pseudo-likelihood scores against h -values, as recommended by the authors (Solís-Lemus et al., 2017).

2.5.2 | D-statistics

We used four-taxon ABBA/BABA tests based on the D -statistic to test for introgression as an explanation for conflicting phylogenetic relationships (Durand et al., 2011). Briefly, for the sister species P1 and P2 (i.e., *P. cantabricae* and *P. carpetana*, respectively), which diverged from a common ancestor with P3 (i.e., *P. pedestris*), and the outgroup O (i.e., *C. pyrenaea*), the D -statistic is used to test the null hypothesis of no introgression ($D = 0$) between P3 and P1 or P2. D -values significantly different from zero indicate gene flow between P1 and P3 ($D < 0$) or between P2 and P3 ($D > 0$). We performed ABBA/BABA tests in PYRAD and used 1000 bootstrap replicates to obtain the standard deviation of the D -statistic and significance levels (Eaton & Ree, 2013). We ran ABBA/BABA tests sequentially for each of the six different species-population combinations (i.e., using each population as a representative for a species). Only populations with six or more genotyped individuals were considered for these analyses (see Table S1). We ran these analyses using six different genetic data sets obtained by setting different clustering thresholds ($W_{\text{clust}} = 0.85$ and 0.90) and minimum taxon coverage for a given locus ($\text{minCov} = 10, 20$ and 30).

2.5.3 | Population graphs

We analysed the potential presence of introgression and determined the direction of gene flow using TREEMIX version 1.12 (Pickrell & Pritchard, 2012). TREEMIX fits a population graph based on population allele frequencies and a Gaussian approximation to genetic drift, inferring patterns of splits and admixtures. We ran TREEMIX analyses considering the same six species-population combinations used for ABBA/BABA tests, assuming independence of all SNPs with a window size of one SNP ($k = 1$). Using an estimated ML tree rooted with the outgroup *C. pyrenaea*, we tested a range of migration events (m from 0 to 4) and determined the best fit model for the data by plotting $\text{Ln}(\text{likelihood})$ scores against m -values.

2.5.4 | Models of interspecific gene flow

We used FASTSIMCOAL2 (Excoffier et al., 2013) to evaluate the fit of the data to 10 alternative divergence models that considered different scenarios of interspecific gene flow (see Figure S1); the timing of gene flow was modelled as a time interval, with an estimate for the time gene flow was initiated (T_{INTROG1}) and the time that it ended (T_{INTROG2} ; Figure S1). We estimated the composite likelihood of the observed data (analysing one SNP per locus) given a specified model using the site frequency spectrum (SFS) and the

simulation-based approach implemented in *FASTSIMCOAL2* (Excoffier et al., 2013). Separate analyses of one population per species were performed considering six different species–population combinations, as done for ABBA/BABA tests and *TREEMIX* analyses. Because invariable sites were not included in the SFS, we fixed the effective population size for one species (*P. cantabrigae*) to enable the estimation of other parameters in *FASTSIMCOAL2* (Excoffier et al., 2013); the fixed effective population size was calculated from the level of nucleotide diversity ($\pi = 0.0005$) and the mutation rate per site per generation (2.8×10^{-9}) estimated for *Drosophila melanogaster* (Keightley et al., 2014), which is similar to the spontaneous mutation rate estimated for the butterfly *Heliconius melpomene* (2.9×10^{-9} ; Keightley et al., 2015). To remove all missing data for the calculation of the joint SFS (as required), each population group was downsampled to five individuals using the *easySFS.py* script (I. Overcast, <https://github.com/isaacovercast/easySFS>).

Each model was run 100 replicated times considering 100,000–250,000 simulations for the calculation of the composite likelihood, 10–40 expectation–conditional maximization (ECM) cycles, and a stopping criterion of 0.001 (Excoffier et al., 2013). We used an information-theoretic model selection approach based on Akaike's information criterion (AIC) to determine the probability of each model given the observed data (Burnham & Anderson, 2002). Specifically, AIC values for each model were rescaled (Δ AIC) calculating the difference between the AIC value of each model and the minimum AIC obtained among all competing models (i.e., the best model has Δ AIC = 0; see Thome & Carstens, 2016). Point estimates of the different demographic parameters for the best supported model were selected from the run with the highest maximum composite likelihood, with confidence intervals (based on the percentile method; e.g., de Manuel et al., 2016) calculated from 100 parametric bootstrap replicates of simulated SFS under the maximum composite likelihood parameter estimates (Excoffier et al., 2013).

2.6 | Inference of past demographic history

We reconstructed the past demographic history from the SFS using the program *STAIRWAY PLOT* version 2.1, which does not require whole-genome sequence data or reference genome information (Liu & Fu, 2015, 2020). We computed the SFS for each population as described in the previous section and ran *STAIRWAY PLOT* fitting a flexible multi-epoch demographic model, considering 1 generation per year (Barton & Hewitt, 1981), assuming a mutation rate of 2.8×10^{-9} per site per generation (Keightley et al., 2014), and performing 200 bootstrap replicates to estimate 95% confidence intervals.

2.7 | Environmental niche modelling

We estimated environmental niche models (ENM) to (i) predict the geographical distribution of climatically suitable areas for the

three species both in the present and during the last glacial maximum (LGM, 21 ka) and to (ii) determine if they support historical geographical contact among species (i.e., overlap of predicted distributions), which might explain observed patterns of genetic introgression (see Section 3.4). We used the maximum entropy algorithm implemented in *MAXENT* version 3.3.3 (Phillips et al., 2006; Phillips & Dudik, 2008), the 19 bioclimatic variables from the *WORLDCLIM* data set (<http://www.worldclim.org/>) interpolated to 30-arcsec resolution ($\sim 1\text{-km}^2$ cell size) (Hijmans et al., 2005), and species occurrence data, which included our own collections and records available in the literature and the Global Biodiversity Information Facility (GBIF.org, February 6, 2018, GBIF Occurrence Downloads; *P. pedestris*: <https://doi.org/10.15468/dl.e78df8>; *P. carpetana*: <https://doi.org/10.15468/dl.jy1fiu>; *P. cantabrigae*: <https://doi.org/10.15468/dl.ngt6yi>). We mapped and examined all records to identify and exclude obvious georeferencing errors and duplicate records (i.e., those falling within the same grid cell); this left final data sets of five entries for the narrow endemic *P. cantabrigae*, 36 entries for *P. carpetana* and 34 entries for *P. pedestris*. Although the number of available records is small, particularly for the narrowly distributed *P. cantabrigae*, similar sample sizes have been proven to be enough to develop ENMs with a good predictive power using *MAXENT* (e.g., Papes & Gaubert, 2007; van Proosdij et al., 2016; Wisz et al., 2008). We used the R package *ENMeval* (Muscarella et al., 2014) to conduct species-specific parameter tuning and determine the optimal feature class (FC) and regularization multiplier (RM) settings for *MAXENT* using a delete-one jackknife optimization approach, as recommended for small data sets (Muscarella et al., 2014; Shcheglovitova & Anderson, 2013). We tested a total of 248 models of varying complexity by combining a range of RMs (from 0 to 15 in increments of 0.5) with eight different FC combinations (L, LQ, LQP, H, T, LQH, LQHP and LQHPT, where L = linear, Q = quadratic, H = hinge, P = product and T = threshold) (Muscarella et al., 2014). Model performance was compared using the minimum training presence omission rate (OR_{MTP}) as the primary optimality criterion (to protect against overfitting) and the area under the curve of the receiver-operating characteristic plot on the testing data (AUC_{TEST}) as a secondary criterion (to maximize the discriminatory ability of the model) (see Wachter et al., 2016). We selected model parameters (RM and FC) and the set of environmental variables retained in the final model following the multistep approach detailed in González-Serna et al. (2019). To generate maps with predicted distributions during the Last Glacial Maximum (LGM), we projected species-specific ENMs onto LGM bioclimatic conditions derived from the MIROC-ESM (Model of Interdisciplinary Research on Climate; Hasumi & Emori, 2004) and the CCSM4 (Community Climate System Model; Braconnot et al., 2007) general atmospheric circulation models. Climatically suitable areas for each species and time period were identified by converting the logistic outputs from *MAXENT* into binary maps using the maximum training sensitivity plus specificity (MTSS) threshold value for occurrence (Liu et al., 2005).

3 | RESULTS

3.1 | Genomic data

A total of 42,277,831 (mean \pm SD = 3,019,845 \pm 984,204 reads per individual), 58,328,181 (mean \pm SD = 2,160,303 \pm 929,130 reads per individual), 22,308,056 (mean \pm SD = 3,186,865 \pm 497,316 reads per individual) and 23,824,106 (mean \pm SD = 3,403,443 \pm 568,441 reads per individual) reads were obtained for *Podisma pedestris*, *P. carpetana*, *P. cantabricae* and *Cophopodisma pyrenaica*, respectively. The number of reads retained after the different quality filtering steps averaged 85% (Figure S2) and the final data set contained 23,517 loci, of which 23,333 were variable and contained at least one SNP (mean number of SNPs per RAD locus = 9.49, excluding the outgroup) under a clustering threshold of sequence similarity of 0.85 ($W_{\text{clust}} = 0.85$) and discarding loci in fewer than 20 individuals ($\text{min-Cov} = 20$). All pairs of genotyped individuals had negative relatedness values (ranging from -6.56 to -0.09), which excludes the possibility that we had sampled close relatives (Manichaikul et al., 2010).

3.2 | Quantifying genetic structure

For the STRUCTURE analyses, $\text{LnPr}(X|K)$ plateaued at $K = 3$ and ΔK peaked at the same K -value (Figure S3a), which corresponds to the three taxa, with no sign of genetic admixture among them (i.e., individual and population probabilities of membership = 1; Figure 1a). STRUCTURE analyses performed separately on *P. pedestris* and *P. carpetana* revealed a strong population genetic structure within each species

(Figure 1a). Two genetic clusters inferred for *P. pedestris* (Figure S3b) group individuals by the two analysed populations for this species (AUL and AIG), with no signs of genetic admixture (Figure 1a). For *P. carpetana*, the most likely number of clusters was $K = 2$ according to the ΔK criterion, but $\text{LnPr}(X|K)$ steadily increases up to $K = 4$ (Figure S3c). These analyses reveal a north-south hierarchical genetic structure, with signs of admixture restricted to some nearby populations from the Iberian System (DEM-URB and URB-MON; see Figure 1). PCAs separate well the three taxa and most populations within taxa, supporting the results from STRUCTURE (Figure S4).

3.3 | Phylogenomic inference

The monophyly of all taxa and the same species relationships were estimated by both SNAPP and SVDQUARTETS (Figures 2 and S5). Phylogenetic relationships among species are well supported with SNAPP (posterior probability >0.98; Figure 2a), but not with SVDQUARTETS (Figures 2b and S5), although the estimates from SVDQUARTETS are robust to different schemes of data filtering and assembling (Figure S5). The phylogenetic relationships among geographically proximate populations of *P. carpetana* were not well resolved by either SNAPP or SVDQUARTETS (Figure 2; see also Figure S5). In SNAPP, the three topologies contained in the 95% HPD tree set differed only in the population relationships inferred for *P. carpetana* (Table S2). These unresolved population relationships within *P. carpetana* are not unexpected given evidence of gene flow among nearby populations located in the same mountain range from STRUCTURE (Figure 1a) and PCAs (Figure S4).

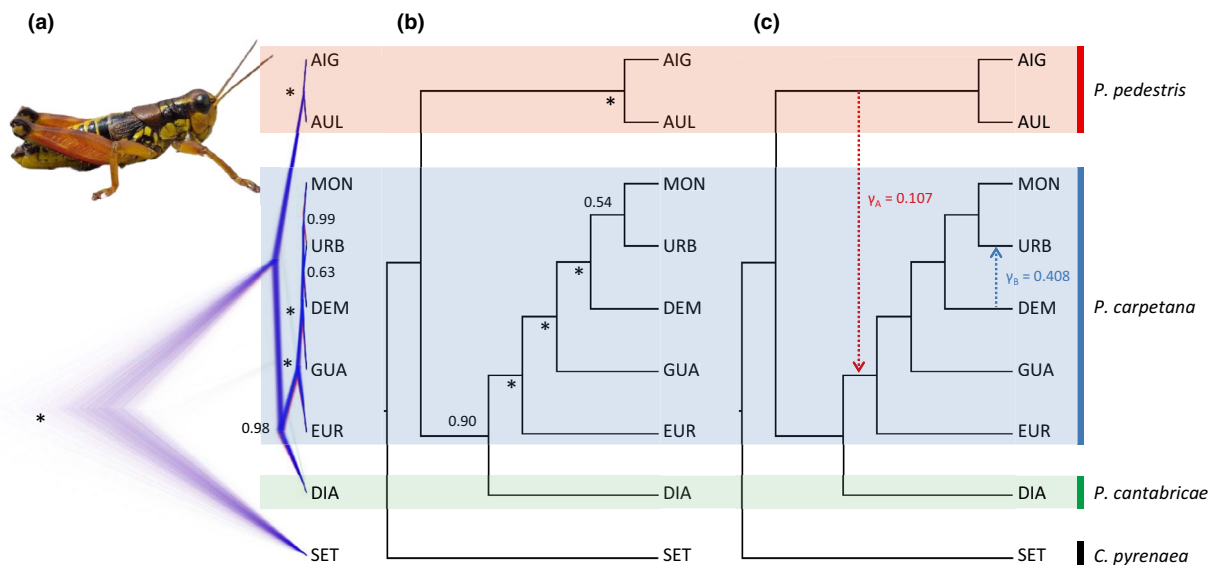


FIGURE 2 Phylogenetic estimates from (a) SNAPP (2287 SNPs), (b) SVDQUARTETS (20,937 SNPs) and (c) PHYLONETWORKS (1447 loci) with the different species demarcated by different shaded colours. Bayesian posterior probabilities (for SNAPP) and bootstrapping support values (for SVDQUARTETS) are indicated on the nodes (* = 1), and the inferred inheritance probabilities (γ_A and γ_B) for each parent are shown on the PHYLONETWORKS tree. Population codes are described in Table S1. Picture shows a male of *Podisma pedestris*, which is morphologically similar to the other two species

3.4 | Analyses of introgression

3.4.1 | Phylogenetic networks

PHYLONETWORK analyses revealed that all models involving reticulation events ($h > 0$) fit our data better than models considering strict bifurcating trees ($h = 0$) (Figure S6). Negative pseudo-likelihood scores decrease sharply from $h = 0$ to $h = 2$ and remain unaltered or with a very small improvement for $h > 2$ (Figure S6), suggesting that the best-fitting phylogenetic model includes two introgression events. One inferred introgression event (γ_A) is from *P. pedestris* into *P. carpetana*, with ~11% of gene copies in the ancestor of *P. carpetana* traced to the ancestor of the two populations of *P. pedestris* (Figure 2c). The other inferred introgression event (γ_B) is from DEM to URB populations of *P. carpetana*, with ~48% of genetic material of population URB originated from DEM (Figure 2c), which is qualitatively similar to the results from STRUCTURE (Figure 1a). The backbone of the tree recovered with PHYLONETWORKS is consistent with those obtained with SNAPP and SVDQUARTETS, differing only in the phylogenetic relationships of some nearby populations of *P. carpetana* from the Iberian System (Figure 2).

3.4.2 | D-statistics

A statistically significant excess of ABBA patterns ($D > 0$) supports post-divergence gene flow between *P. pedestris* (P3) and *P. carpetana* (P2) (Table 1). This result holds irrespective of which population–species combinations were analysed, or the data filtering and assembling scheme used in generating the data set (Table S3).

3.4.3 | Population graphs

TREEMIX analyses consistently support a single migration event (Figure S7) of directional gene flow from *P. pedestris* to *P. carpetana* (Figures 3 and S8).

3.4.4 | Models of interspecific gene flow

FASTSIMCOAL2 analyses performed for all population–species combinations consistently show that the best supported scenario is one with asymmetrical gene flow from *P. pedestris* to *P. carpetana* (Figure 4; Model B in Table S4). Considering the 1-year generation time of these species (Barton & Hewitt, 1981), the split between *P. pedestris* and the two other taxa is estimated to have taken place ~638,000–992,000 years ago, during the early–middle Pleistocene (Figure 4; Table S5). The split between *P. carpetana* and *P. cantabricae* is estimated as ~131,000–155,000 years ago, during the middle Pleistocene (Figure 4; Table S5). Gene flow from *P. pedestris* to *P. carpetana* is inferred to have taken place during the middle–late Pleistocene, between ~108,000–147,000

and 87,000–120,000 years ago (Figure 4; Table S5). It should be noted that estimates for the 95% confidence intervals for the oldest demographic parameters (θ_{ANC} , $\theta_{CAR-CAN}$ and T_{DIV1}) are much wider than those for more recent events (θ_{PED} , θ_{CAR} , T_{DIV2} , $T_{INTROG1}$ and $T_{INTROG2}$) (Figure 4; Table S5), which is consistent with the lower accuracy of FASTSIMCOAL2 to estimate more ancient events, such as those involving species formation (Excoffier et al., 2013).

3.5 | Inference of past demographic history

STAIRWAY PLOT analyses suggest the three species experienced parallel demographic responses to climate warming since the end of the last glacial period (Figure 5). More specifically, all analysed populations from the three species show demographic declines that generally follow the LGM and reduced their effective population sizes (N_e) by >95% (Figure 5). We note that these population size estimates differ from those of the parameterized divergence model (Figure 4), but that the divergence model did not include population size change parameters because of the complexity it would have added to the alternative tested models (Knowles, 2009).

3.6 | Environmental niche modelling

The low OR_{MTP} ($OR_{MTP} < 0.01$) and high AUC_{TEST} ($AUC_{TEST} > 0.99$) for the ENM of each species indicate their high discriminatory power and low degree of overfitting, respectively (for details on model performance and parameters, see Table S6). Climatically suitable areas predicted by ENMs yield distribution patterns highly congruent with the present-day observed distributions for the three species (Figure 6). Only very small areas in mountain ranges far from the current distribution of each species are (over-)predicted as suitable (Figure 6). Palaeoclimatic reconstructions under both the MIROC-ESM and CCSM4 general atmospheric circulation models yield reasonably similar predictions about the distribution of the three species during the LGM (Figure 6), although the extent of the projected distributions varies among the species. Projection of the present-day climate niche envelope to LGM climatic conditions suggests some important changes in the distribution and patterns of population connectivity of the three species (Figure 6). In particular, with a more continuous distribution and overall higher suitability during the LGM than in the present in each species, they are projected to have had considerable overlap in their distributions in the past (Figure 6).

4 | DISCUSSION

Although genetic evidence of reticulate evolution suggests incomplete reproductive isolation among some Iberian *Podisma* grasshoppers in the past, genetic cohesion has been maintained across each species, even in the face of multiple distribution shifts in response to Pleistocene glacial cycles. However, several lines of evidence suggest

TABLE 1 Analyses of introgression using four-taxon *D*-statistic (ABBA/BABA) tests

P1 (<i>P. cantabricae</i>)	P2 (<i>P. carpetana</i>)	P3 (<i>P. pedestris</i>)	<i>n</i>	BABA	ABBA	<i>D</i> (\pm SD)	<i>z</i>	<i>q</i>
DIA	EUR	AUL	3772	595	932	0.221 \pm 0.031	7.08	<.001
DIA	MON	AUL	3601	546	990	0.289 \pm 0.031	9.29	<.001
DIA	GUA	AUL	3553	577	948	0.244 \pm 0.033	7.45	<.001
DIA	EUR	AIG	3808	592	961	0.238 \pm 0.031	7.70	<.001
DIA	MON	AIG	3640	551	1026	0.301 \pm 0.031	9.86	<.001
DIA	GUA	AIG	3587	566	962	0.259 \pm 0.031	8.46	<.001

Note: Analyses were performed for each of the six species–population combinations separately using *Cophopodisma pyrenaica* as an outgroup. All tests were highly significant ($q < .001$) after a false discovery rate (FDR) adjustment (5%) to control for multiple tests. Population codes are described in Table S1. *n*, number of retained SNPs; *D* (\pm SD), *D*-statistic and corresponding standard deviation; *z*, *z*-statistic; *q*, *p*-values adjusted at a FDR of 5%.

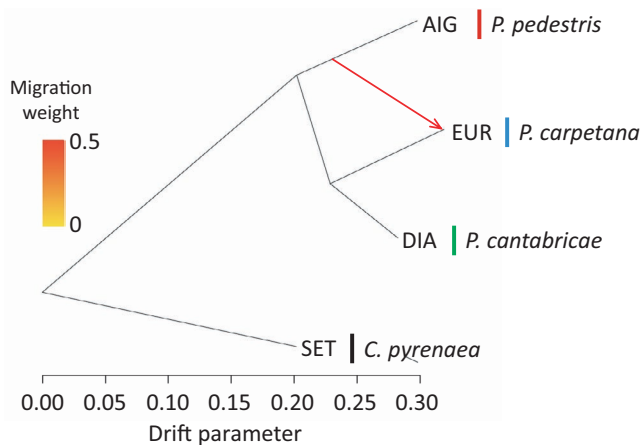


FIGURE 3 Maximum-likelihood tree inferred with TREEMIX (4569 SNPs) showing the most likely migration event ($m = 1$). The direction of gene flow is represented with an arrow coloured according to the percentage of alleles (weight) originating from the source. Codes of the specific populations of each species included in the analysis are described in Table S1. Note that analogous TREEMIX analyses were run considering all other species–population combinations (see Figure S8)

that this is not due solely to the rapid evolution of reproductive isolation. Instead, the spatial distribution of sky islands, along with limited dispersal capacity and marked population declines during interglacial periods, may be important factors in maintaining geographical isolation in the face of climate-induced distributional shifts. These insights are only apparent when considering a suite of analyses in which each unveils an aspect of the speciation process, but together convey how divergence across a complex landscape during a dynamic historical period of climate change might have taken place, avoiding a melting-pot scenario in which gene flow precludes speciation.

4.1 | Determinants of species pump or melting-pot processes

In areas with temperate climates, such as the Mediterranean region, cold-adapted species with narrow climatic niches are currently

limited to small and isolated patches of high-elevation habitat (i.e., sky islands; Flantua et al., 2020; Knowles & Massatti, 2017). Fragmentation of contemporary populations is clearly reflected in patterns of genetic structure within the studied species complex, with all assigned to a unique genetic cluster with a high probability (>0.99) of membership, except for three nearby populations (DEMA, URBI and MON) of *Podisma carpetana* from the same mountain range (Figure 1). However, during past glacial periods when lower temperatures predominated, the expansion of temperate climatic conditions into what is now unsuitable habitat is also predicted to have driven expansion of cold-adapted species (Hewitt, 2000). Accordingly, range expansions during glacial periods and extreme contractions during interglacials (i.e., current conditions) were inferred in each of the *Podisma* species from ENMs (Figure 6). These inferences are corroborated by genomic-based demographic reconstructions that show marked, parallel declines in the population size of each species starting around the onset of the Holocene (Figure 5). Postglacial demographic bottlenecks were dramatic, with effective population sizes reduced to a fraction of those estimated around the LGM. This is consistent with the current distribution of climatically suitable habitats and the low dispersal capability of the species that nowadays persist in small and highly fragmented interglacial refugia (Bennett & Provan, 2008; Stewart et al., 2010). Thus, both extreme isolation and severe demographic bottlenecks after the LGM created the perfect scenario for genetic differentiation via strong genetic drift and a fragmented population structure.

In the different sky island archipelagos of the Iberian Peninsula, like other montane regions across the globe, the repeated climate-induced distributional shifts and associated demographic conditions (e.g., bottlenecked and fragmented populations) experienced by their biotas represent the quintessential setting for a species pump diversification process (Flantua et al., 2020; Haffer, 1969; Papadopoulou & Knowles, 2015a; Wallis et al., 2016). However, this dynamic can transition into a melting-pot scenario—that is, the repeated cycles of distributional shifts result in the loss of incipient divergences due to gene flow during range expansions (Klicka & Zink, 1997; Maier et al., 2019). This tipping point between distributional shifts promoting vs. inhibiting speciation is expected to vary among species and geographical settings. The inherent dispersal constraints of flightlessness, coupled with climatic adaptation

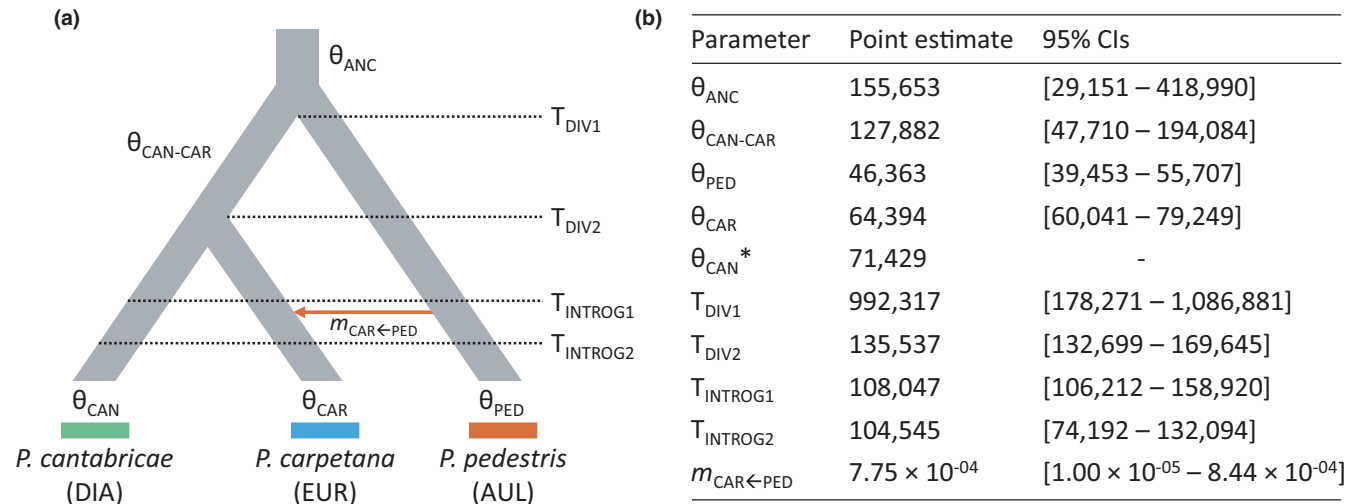


FIGURE 4 Demographic parameters inferred with FASTSIMCOAL2 for the most likely species divergence model (Model B, a divergence with gene flow model; see Tables S4 and S5). Table shows point estimates and lower and upper 95% confidence intervals (in brackets) for each parameter: the ancestral (θ_{ANC} , $\theta_{CAN-CAR}$) and contemporary (θ_{PED} , θ_{CAR} , θ_{CAN}) effective population sizes, migration rates (m), timing of species split (T_{DIV1} , T_{DIV2}) and timing (beginning and end) of interspecific gene flow ($T_{INTROG1}$, $T_{INTROG2}$), with time given in units of generations (or years, with one generation per year). Codes of the specific populations (AUL, EUR and DIA) of each species included in the analysis are described in Table S1. Parameter estimates for analogous FASTSIMCOAL2 analyses run considering all other species–population combinations are presented in Table S5. *Note the effective population size of *Podisma cantabricae* (θ_{CAN}) was calculated from the level of nucleotide diversity (π) and fixed in FASTSIMCOAL2 analyses (see the Section 2.5.4 for further details)

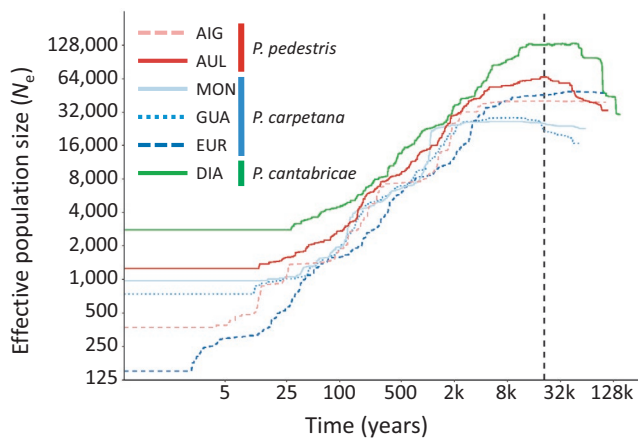


FIGURE 5 Demographic history of the studied populations of *Podisma pedestris*, *P. carpetana* and *P. cantabricae* inferred using STAIRWAY PLOT (only populations with six or more genotyped individuals were analysed). Panels show the median of effective population size (N_e) over time, estimated assuming a mutation rate of 2.8×10^{-9} and 1-year generation time (both axes on a logarithmic scale). Vertical dashed line indicates the Last Glacial Maximum (LGM; ~21,000 years ago). Population codes are described in Table S1

of *Podisma* grasshoppers to montane and alpine environments, suggests species' traits may indeed contribute to the relative isolation and demographic bottlenecks that promote and maintain genetic differentiation (Papadopoulou & Knowles, 2016; e.g., Ortego et al., 2015; Papadopoulou & Knowles, 2015b; Schoville et al., 2012; Thomaz & Knowles, 2020). With closely related species of insects often distinguished only by male genitalia, it also suggests that

sexual selection may play a role in maintaining species boundaries and explain limited hybridization among the studied species during periods of extensive secondary contact (Arnqvist, 1998; Hosken & Stockley, 2004; also see Marquez & Knowles, 2007 for an example in montane grasshoppers in North America). However, biotic factors are not the only determinant of the fate of incipient divergences. The geographical context of climatic-induced distributional shifts of habitats and their constituent inhabitants are also important. That is, the dynamics of colonization itself may be instrumental in determining the distribution of genetic variation and differentiation (see Knowles & Massatti, 2017).

With the sky islands in the Iberian Peninsula embedded in a landscape of unsuitable habitat, the likelihood of dispersal may certainly be reduced, but not impossible, especially with the projections of a more expansive distribution of suitable habitat for temperate taxa in the past (Figure 6). Yet, the presence of past corridors of suitable habitat among the isolated contemporary populations does not necessarily mean that they were utilized or that the three *Podisma* species actually came into secondary contact. Low dispersal ability and a marked philopatric behaviour of these flightless species (Barton & Hewitt, 1981, 1982; Mason et al., 1995), ecological constraints (e.g., biotic interactions; Hampe, 2004; Ortego & Knowles, 2020), and the strong fragmentation and small sizes of severely bottlenecked populations (Figures 1 and 5) might have hampered their capacity to colonize remote areas that were climatically suitable during glacial periods (Kearney & Porter, 2009; Wiens et al., 2009). For instance, it is likely that the current tiny distribution of *P. cantabricae* (<25–50 km²; Presa et al., 2016b) in a topographically highly complex region severely limited its capacity to reach predicted environmentally suitable, but

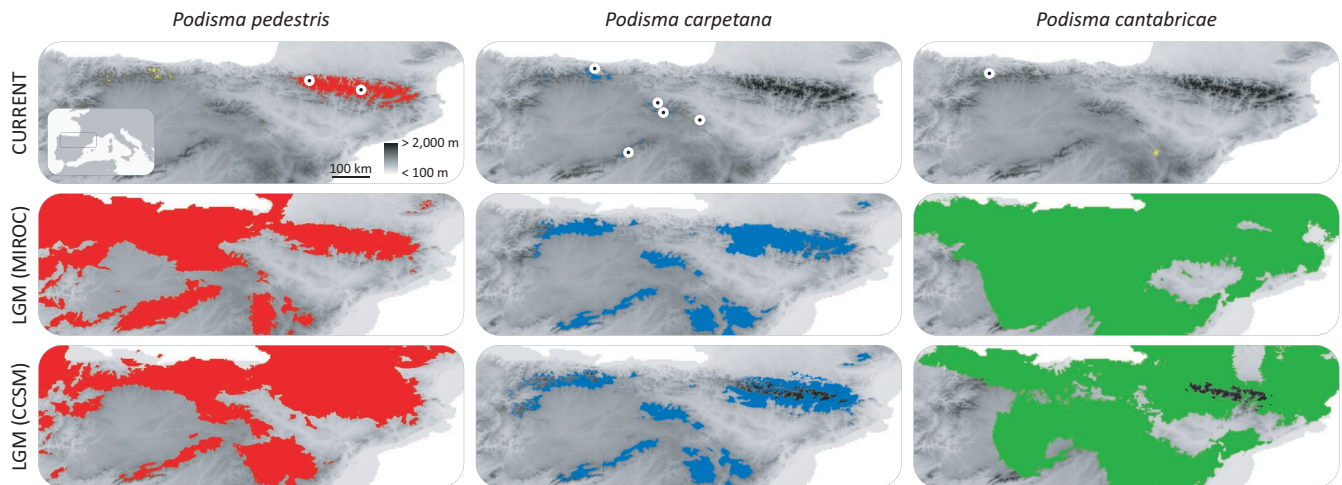


FIGURE 6 Current and Last Glacial Maximum (LGM) distributions for each species as predicted by environmental niche models (ENMs). Colours indicate areas predicted to be occupied by each species according to the maximum training sensitivity plus specificity (MTSS) logistic threshold of their respective ENM (Table S6). Predicted distributions for the LGM are based on the MIROC-ESM and the CCSM4 general atmospheric circulation models. Elevation is shown by grey shading, with darker areas corresponding to higher elevations. Yellow colour in current distribution maps indicate small areas (barely visible) predicted as suitable by ENMs but located outside the known distribution ranges of each species (i.e., over-predictions). Current distribution maps show sampling localities (black dots with white rings) for each species; the small map inset shows the position of the species distribution on the Iberian Peninsula

distant areas (i.e., located > 1000 km away from its current range) during the LGM (Figure 6). In sum, incipient divergences may be lost among some sky island populations, but not others, and similarly, the opportunity for past hybridization among currently allopatric *Podisma* taxa may depend on the contemporary and past geographical configuration of suitable habitats within the dynamic ranges of each species (Knowles & Massatti, 2017; Tonzo & Ortego, 2021).

When the speciation process is viewed through the lens of divergence with gene flow, rather than divergence in isolation, it invites a shift in perspective about the controls on speciation (Aguilée et al., 2018; Harvey et al., 2019). For example, in addition to the traditional focus on the rate of evolution of reproductive isolation as a control on diversification (in which potential gene flow associated with cycles of climate-induced distributional shifts is thwarted), given that divergence in *Podisma* does not fit a divergence in isolation model (Figures 3 and 4), other factors may be involved in the maintenance of incipient divergence. Both the differences in the relative timing of divergence, as well as differences in inferred gene flow among *Podisma* species and population lineages (Figures 2–4), point to varying degrees in the permeability of lineage boundaries. This suggests that the differing consequences of hybridization (i.e., the varied possibilities and effects of gene flow) across the landscape may control diversification dynamics. That is, opportunities and extent of gene flow across the landscape may determine whether repeated distributional shifts act as a species-pump vs. a melting pot, not just the rate of reproductive isolation (Aguilée et al., 2018; Dynesius & Jansson, 2014; Harvey et al., 2019).

From this perspective of divergence with gene flow (as opposed to divergence in isolation), in which the rate of reproductive isolation is not the only factor controlling diversification, the timing of

divergence can take on new meaning and provide new insights into the speciation process. It is notable that species boundaries are maintained even though some have remained semipermeable for extended periods of time (i.e., introgression between nonsister species *P. pedestris* and *P. carpetana*; Figure 4). In other words, reproductive isolation may be viewed as having been more or less effective in reducing the loss of incipient divergences, especially given that projections of species distributions predict some overlap among all *Podisma* species during glacial periods. In addition, because these past distributions were not contiguous, but rather some dispersal corridors were more limited in geographical scope than others (Figure 6), it suggests that the opportunities for gene flow (or, conversely, the extent of geographical isolation) may have had a prominent effect on the permeability of species boundaries, in addition to any role the rate of reproductive isolation might have played in speciation. In fact, while we cannot exclude the possibility that the rate of evolution of reproductive isolation as a key determinant of the likelihood of speciation (as well as the genetic cohesion of all the species), we can make an argument that Pleistocene speciation in *Podisma* grasshoppers probably had other contributing factors. For example, if speciation was indeed promoted by the fragmentation and isolation of populations during the relatively short interglacial periods, rather than the geologically longer glacial periods when the grasshopper distributions are projected to have been more widespread (Figure 6), it would imply the development of reproductive isolating mechanisms correspondingly much more rapid than in classical models where displacements into isolated glacial refugia promoted speciation (e.g., Hewitt, 1996; Knowles, 2001; also see Klicka & Zink, 1997; Ebdon et al., 2021 for arguments against Pleistocene speciation because of the rapidity of glacial cycles).

4.2 | Determinants of permeable species boundaries

Although ENMs predicted that the distributions of the three taxa largely overlapped during the LGM, genomic data only supported gene flow from *P. pedestris* and *P. carpetana*. Different reasons could explain this specific history of limited introgressive hybridization. Lack of historical hybridization between some species pairs might be a consequence of limited past connectivity and opportunity for gene flow due to geographical isolation (i.e., the geographically distant contemporary ranges of *P. pedestris* and *P. cantabricae*; Figure 1). Alternatively, some of the studied species might have quickly evolved pre- or postzygotic reproductive isolation mechanisms (i.e., speciation in strict isolation) as a by-product of allopatric divergence (Coyne & Orr, 2004) or via reinforcement after secondary contact (Pfennig, 2016; Servedio & Noor, 2003). For instance, the two sister species *P. carpetana* and *P. cantabricae* currently have geographically adjacent distributions in northwestern Iberia (Figure 1), and multiple instances of secondary contact during the estimated distributional expansions (Figure 6) might have accelerated the rapid evolution of reproductive isolation (Coyne & Orr, 2004; Hoskin et al., 2005). Accordingly, previous studies have found that hybrid dysfunction, genetic incompatibilities and the evolution of pre- and postzygotic reproductive isolation mechanisms is frequent in contact zones between species (Bailey et al., 2004), subspecies (Virdee & Hewitt, 1994) and chromosomal races (Barton & Hewitt, 1981) of montane and alpine grasshoppers.

An intriguing finding is that historical gene flow between *P. pedestris* and *P. carpetana* was asymmetric (Figures 2–4). Unidirectional introgression might have resulted from extensive hybridization during periods of secondary contact followed by repeated backcrossing between hybrids and only one parental species (e.g., Field et al., 2011; Kirschel et al., 2020). Asymmetric gene flow could also be explained by a higher capacity of the donor species to disperse into the range of the recipient one (Jacquemyn et al., 2012; Ortego et al., 2021). In the absence of reproductive barriers, the two species will interbreed and first-generation hybrids will more often mate with the most abundant local species, resulting in introgressive hybridization. Although *P. pedestris* is generally a micropterous flightless species, long-winged individuals have been frequently described in the literature (Lemonnier-Darcemont & Darcemont, 2014 and references therein) and this polymorphism has been suggested to favour population connectivity and contribute to the colonization of suitable habitats (Zuna-Kratky et al., 2016). In contrast, the two other *Podisma* species from the Iberian Peninsula are either apterous (*P. cantabricae*) or micropterous (*P. carpetana*) and long-winged forms have never been reported (Morales-Agacino, 1951; Presa et al., 2016a, 2016b). In Orthoptera species presenting wing polymorphism, macropterous forms seem to be occasional and occur at low frequencies within populations. However, these forms have been found to be integral for range expansions at extremely short spatiotemporal scales (Hochkirch & Damerou, 2009), which might be particularly exacerbated under changing environmental conditions

such as those imposed by Quaternary climatic oscillations (Simmons & Thomas, 2004). In the context of our study, increased availability of suitable habitats for colonization in the transition from interglacial to glacial periods might have led to selection for macropterous forms in peripheral populations at the expanding margins and favoured dispersal of *P. pedestris* into the distribution range of *P. carpetana* (Hochkirch & Damerou, 2009; Nogueras et al., 2016).

5 | CONCLUSIONS

Our integrative analyses have provided limited evidence of inter-specific gene flow during prolonged periods of projected extensive secondary contact and emphasize the genetic cohesiveness of all species within the alpine *Podisma* complex. These findings support the notion that the interplay among Pleistocene-driven isolation (i.e., confinement in interglacial refugia), landscape composition (i.e., spatial configuration of sky islands), and species' traits (i.e., flightlessness) can trigger the necessary mechanisms for long-lasting genomic diversification and speciation in alpine and montane biotas (Dynesius & Jansson, 2014; Knowles, 2001). Our comprehensive suite of distributional, demographic and phylogenomic analyses also provide a mechanistic explanation for the uncertain phylogenetic relationships among the studied grasshopper species and collectively highlight the important role of Quaternary climatic oscillations in promoting diversification and genetic fragmentation of relictual alpine organisms from temperate regions that currently persist as highly isolated populations in disparate mountain ranges. Irrespective of which factors control diversification (i.e., the rate of reproductive isolation vs. dispersal, and hence opportunities for gene flow), the time of speciation supports a model of Pleistocene divergence. This, in its own right, means that *Podisma* grasshoppers of the sky islands from the Iberian Peninsula constitute an ideal system to further investigate some intriguing questions that the different independent data types and analytical procedures raise about the speciation process. Future experimental crosses might reveal the presence of pre- and postzygotic barriers to interspecific gene flow that could clarify whether the absence of genomic evidence for introgressive hybridization among most species-pairs is a consequence of reproductive isolation and the completion of the speciation process or resulted from limited opportunity for hybridization due to population isolation in sky islands and dispersal constraints during range expansions.

ACKNOWLEDGEMENTS

We thank Amparo Hidalgo-Galiana for library preparation, Víctor Nogueras and Pedro J. Cordero for collecting samples from Picos de Europa, Vanina Tonzo and Anna Papadopoulou for help during fieldwork and data analysis, Sergio Pereira (The Centre for Applied Genomics) for Illumina sequencing, and three anonymous referees for their constructive and valuable comments on an earlier version of the manuscript. We thank Spanish and French National Parks

and the environmental authorities from each region for providing sampling permissions. We also thank Laboratorio de Ecología Molecular from Estación Biológica de Doñana (LEM-EBD) for logistical support and Centro de Supercomputación de Galicia (CESGA) and Doñana's Singular Scientific-Technical Infrastructure (ICTS-RBD) for access to computer resources. Research was funded by the Spanish Ministry of Economy, Industry and Competitiveness and European Social Fund (grant nos.: CGL2014-54671-P and CGL2017-83433-P).

CONFLICT OF INTEREST

The authors have no conflicts of interest to declare.

AUTHOR CONTRIBUTIONS

J.O. and L.L.K. conceived the study and designed the research. J.O. collected the samples and produced and analysed the data. J.O. led the writing with inputs from L.L.K.

DATA AVAILABILITY STATEMENT

Raw Illumina reads have been deposited at the NCBI Sequence Read Archive (SRA) under BioProject PRJNA759248. Input files for all analyses are available for download on Figshare (<https://doi.org/10.6084/m9.figshare.16645912>).

ORCID

Joaquín Ortego  <https://orcid.org/0000-0003-2709-429X>

L. Lacey Knowles  <https://orcid.org/0000-0002-6567-4853>

REFERENCES

- Aguilée, R., Gascuel, F., Lambert, A., & Ferriere, R. (2018). Clade diversification dynamics and the biotic and abiotic controls of speciation and extinction rates. *Nature Communications*, 9, 3013. <https://doi.org/10.1038/s41467-018-05419-7>
- April, J., Hanner, R. H., Dion-Côté, A. M., & Bernatchez, L. (2013). Glacial cycles as an allopatric speciation pump in north-eastern American freshwater fishes. *Molecular Ecology*, 22(2), 409–422. <https://doi.org/10.1111/mec.12116>
- Arnqvist, G. (1998). Comparative evidence for the evolution of genitalia by sexual selection. *Nature*, 393(6687), 784–786. <https://doi.org/10.1038/31689>
- Bailey, R. I., Thomas, C. D., & Butlin, R. K. (2004). Premating barriers to gene exchange and their implications for the structure of a mosaic hybrid zone between *Chorthippus brunneus* and *C. jacobsi* (Orthoptera: Acrididae). *Journal of Evolutionary Biology*, 17(1), 108–119. <https://doi.org/10.1046/j.1420-9101.2003.00648.x>
- Barton, N. H. (1980). The fitness of hybrids between two chromosomal races of the grasshopper *Podisma pedestris*. *Heredity*, 45, 47–59. <https://doi.org/10.1038/hdy.1980.49>
- Barton, N. H., & Hewitt, G. M. (1981). A chromosomal cline in the grasshopper *Podisma pedestris*. *Evolution*, 35(5), 1008–1018. <https://doi.org/10.2307/2407871>
- Barton, N. H., & Hewitt, G. M. (1982). A measurement of dispersal in the grasshopper *Podisma pedestris* (Orthoptera, Acrididae). *Heredity*, 48, 237–249. <https://doi.org/10.1038/hdy.1982.29>
- Bennett, K. D., & Provan, J. (2008). What do we mean by refugia? *Quaternary Science Reviews*, 27(27–28), 2449–2455. <https://doi.org/10.1016/j.quascirev.2008.08.019>
- Bernardes, J. S., Dávila, A. M., Costa, V. S., & Zaverucha, G. (2007). Improving model construction of profile HMMs for remote homology detection through structural alignment. *BMC Bioinformatics*, 8, 435. <https://doi.org/10.1186/1471-2105-8-435>
- Bouckaert, R. R. (2010). DENSITREE: Making sense of sets of phylogenetic trees. *Bioinformatics*, 26(10), 1372–1373. <https://doi.org/10.1093/bioinformatics/btq110>
- Bouckaert, R., Heled, J., Kühnert, D., Vaughan, T., Wu, C.-H., Xie, D., Suchard, M. A., Rambaut, A., & Drummond, A. J. (2014). BEAST2: A software platform for Bayesian evolutionary analysis. *PLoS Computational Biology*, 10(4), e1003537. <https://doi.org/10.1371/journal.pcbi.1003537>
- Braconnot, P., Otto-Bliesner, B., Harrison, S., Joussaume, S., Peterchmitt, J.-Y., Abe-Ouchi, A., Crucifix, M., Driesschaert, E., Fichefet, T. H., Hewitt, C. D., Kageyama, M., Kitoh, A., Laine, A., Loutre, M.-F., Marti, O., Merkel, U., Ramstein, G., Valdes, P., Weber, S. L., ... Zhao, Y. (2007). Results of PMIP2 coupled simulations of the Mid-Holocene and Last Glacial Maximum – Part 1: Experiments and large-scale features. *Climate of the Past*, 3(2), 261–277. <https://doi.org/10.5194/cp-3-261-2007>
- Bryant, D., Bouckaert, R., Felsenstein, J., Rosenberg, N. A., & RoyChoudhury, A. (2012). Inferring species trees directly from biallelic genetic markers: Bypassing gene trees in a full coalescent analysis. *Molecular Biology and Evolution*, 29(8), 1917–1932. <https://doi.org/10.1093/molbev/mss086>
- Burnham, K. P., & Anderson, D. R. (2002). *Model selection and multimodel inference: A practical information-theoretic approach*. Springer.
- Capella-Gutiérrez, S., Silla-Martínez, J. M., & Gabaldón, T. (2009). TRIMAL: A tool for automated alignment trimming in large-scale phylogenetic analyses. *Bioinformatics*, 25(15), 1972–1973. <https://doi.org/10.1093/bioinformatics/btp348>
- Carstens, B. C., & Knowles, L. L. (2007). Shifting distributions and speciation: Species divergence during rapid climate change. *Molecular Ecology*, 16(3), 619–627. <https://doi.org/10.1111/j.1365-294X.2006.03167.x>
- Catchen, J., Hohenlohe, P. A., Bassham, S., Amores, A., & Cresko, W. A. (2013). STACKS: An analysis tool set for population genomics. *Molecular Ecology*, 22(11), 3124–3140. <https://doi.org/10.1111/mec.12354>
- Chifman, J., & Kubatko, L. (2014). Quartet inference from SNP data under the coalescent model. *Bioinformatics*, 30(23), 3317–3324. <https://doi.org/10.1093/bioinformatics/btu530>
- Cigliano, M. M., Braun, H., Eades, D. C., & Otte, D. (2021). *Orthoptera Species File (OSF)*. <http://orthoptera.speciesfile.org>
- Coyne, J. A., & Orr, H. A. (2004). *Speciation*. Sinauer.
- Danecek, P., Auton, A., Abecasis, G., Albers, C. A., Banks, E., DePristo, M. A., Handsaker, R. E., Lunter, G., Marth, G. T., Sherry, S. T., McVean, G., & Durbin, R. (2011). The variant call format and VCFtools. *Bioinformatics*, 27(15), 2156–2158. <https://doi.org/10.1093/bioinformatics/btr330>
- de Manuel, M., Kuhlwilm, M., Frandsen, P., Sousa, V. C., Desai, T., Prado-Martinez, J., Hernandez-Rodriguez, J., Dupanloup, I., Lao, O., Hallast, P., Schmidt, J. M., Heredia-Genestar, J. M., Benazzo, A., Barbujani, G., Peter, B. M., Kuderna, L. F. K., Casals, F., Angedakin, S., Arandjelovic, M., ... Marques-Bonet, T. (2016). Chimpanzee genomic diversity reveals ancient admixture with bonobos. *Science*, 354(6311), 477–481. <https://doi.org/10.1126/science.aag2602>
- Durand, E. Y., Patterson, N., Reich, D., & Slatkin, M. (2011). Testing for ancient admixture between closely related populations. *Molecular Biology and Evolution*, 28(8), 2239–2252. <https://doi.org/10.1093/molbev/msr048>
- Dynesius, M., & Jansson, R. (2014). Persistence of within-species lineages: A neglected control of speciation rates. *Evolution*, 68(4), 923–934. <https://doi.org/10.1111/evo.12316>

- Earl, D. A., & vonHoldt, B. M. (2012). STRUCTURE HARVESTER: A website and program for visualizing STRUCTURE output and implementing the Evanno method. *Conservation Genetics Resources*, 4(2), 359–361. <https://doi.org/10.1007/s12686-011-9548-7>
- Eaton, D. A. R. (2014). PYRAD: Assembly of *de novo* RADseq loci for phylogenetic analyses. *Bioinformatics*, 30(13), 1844–1849. <https://doi.org/10.1093/bioinformatics/btu121>
- Eaton, D. A. R., & Ree, R. H. (2013). Inferring phylogeny and introgression using RADseq data: An example from flowering plants (*Pedicularis: Orobanchaceae*). *Systematic Biology*, 62(5), 689–706. <https://doi.org/10.1093/sysbio/syt032>
- Ebdon, S., Laetsch, D. R., Dapporto, L., Hayward, A., Ritchie, M. G., Dincă, V., Vilá, R., & Lohse, K. (2021). The Pleistocene species pump past its prime: Evidence from European butterfly sister species. *Molecular Ecology*, 30(14), 3575–3589. <https://doi.org/10.1111/mec.15981>
- Evanno, G., Regnaut, S., & Goudet, J. (2005). Detecting the number of clusters of individuals using the software STRUCTURE: A simulation study. *Molecular Ecology*, 14(8), 2611–2620. <https://doi.org/10.1111/j.1365-294X.2005.02553.x>
- Excoffier, L., Dupanloup, I., Huerta-Sánchez, E., Sousa, V. C., & Foll, M. (2013). Robust demographic inference from genomic and SNP data. *PLoS Genetics*, 9(10), e1003905. <https://doi.org/10.1371/journal.pgen.1003905>
- Field, D. L., Ayre, D. J., Whelan, R. J., & Young, A. G. (2011). Patterns of hybridization and asymmetrical gene flow in hybrid zones of the rare *Eucalyptus aggregata* and common *E. rubida*. *Heredity*, 106(5), 841–853. <https://doi.org/10.1038/hdy.2010.127>
- Flantua, S. G. A., Payne, D., Borregaard, M. K., Beierkuhnlein, C., Steinbauer, M. J., Dullinger, S., Essl, F., Irl, S. D. H., Kienle, D., Kreft, H., Lenzner, B., Norder, S. J., Rijdsdijk, K. F., Rumpf, S. B., Weigelt, P., & Field, R. (2020). Snapshot isolation and isolation history challenge the analogy between mountains and islands used to understand endemism. *Global Ecology and Biogeography*, 29(10), 1651–1673. <https://doi.org/10.1111/geb.13155>
- Gilbert, K. J., Andrew, R. L., Bock, D. G., Franklin, M. T., Kane, N. C., Moore, J. S., & Vines, T. H. (2012). Recommendations for utilizing and reporting population genetic analyses: The reproducibility of genetic clustering using the program STRUCTURE. *Molecular Ecology*, 21(20), 4925–4930. <https://doi.org/10.1111/j.1365-294X.2012.05754.x>
- González-Serna, M. J., Cordero, P. J., & Ortego, J. (2019). Spatiotemporally explicit demographic modelling supports a joint effect of historical barriers to dispersal and contemporary landscape composition on structuring genomic variation in a red-listed grasshopper. *Molecular Ecology*, 28(9), 2155–2172. <https://doi.org/10.1111/mec.15086>
- Haffer, J. (1969). Speciation in Amazonian forest birds. *Science*, 165(3889), 131–137. <https://doi.org/10.1126/science.165.3889.131>
- Hampe, A. (2004). Bioclimate envelope models: What they detect and what they hide. *Global Ecology and Biogeography*, 13(5), 469–471. <https://doi.org/10.1111/j.1466-822X.2004.00090.x>
- Harvey, M. G., Singhal, S., & Rabosky, D. L. (2019). Beyond reproductive isolation: Demographic controls on the speciation process. *Annual Review of Ecology, Evolution, and Systematics*, 50, 75–95. <https://doi.org/10.1146/annurev-ecolsys-110218-024701>
- Hasumi, H., & Emori, S. (2004). *K-1 Coupled GCM (MIROC) Description*. Center for Climate System Research (CCSR), University of Tokyo; National Institute for Environmental Studies (NIES); Frontier Research Center for Global Change (FRCGC).
- Hewitt, G. M. (1996). Some genetic consequences of ice ages, and their role in divergence and speciation. *Biological Journal of the Linnean Society*, 58(3), 247–276. <https://doi.org/10.1006/bijl.1996.0035>
- Hewitt, G. (2000). The genetic legacy of the Quaternary ice ages. *Nature*, 405(6789), 907–913.
- Hijmans, R. J., Cameron, S. E., Parra, J. L., Jones, P. G., & Jarvis, A. (2005). Very high resolution interpolated climate surfaces for global land areas. *International Journal of Climatology*, 25(15), 1965–1978. <https://doi.org/10.1002/joc.1276>
- Hochkirch, A., & Damerau, M. (2009). Rapid range expansion of a wing-dimorphic bush-cricket after the 2003 climatic anomaly. *Biological Journal of the Linnean Society*, 97(1), 118–127. <https://doi.org/10.1111/j.1095-8312.2008.01199.x>
- Hosken, D. J., & Stockley, P. (2004). Sexual selection and genital evolution. *Trends in Ecology & Evolution*, 19(2), 87–93. <https://doi.org/10.1016/j.tree.2003.11.012>
- Hoskin, C. J., Higgie, M., McDonald, K. R., & Moritz, C. (2005). Reinforcement drives rapid allopatric speciation. *Nature*, 437(7063), 1353–1356. <https://doi.org/10.1038/nature04004>
- Huang, H. T., & Knowles, L. L. (2016). Unforeseen consequences of excluding missing data from next-generation sequences: Simulation study of RAD sequences. *Systematic Biology*, 65(3), 357–365. <https://doi.org/10.1093/sysbio/syu046>
- Jacquemyn, H., Brys, R., Honnay, O., & Roldán-Ruiz, I. (2012). Asymmetric gene introgression in two closely related *Orchis* species: Evidence from morphometric and genetic analyses. *BMC Evolutionary Biology*, 12, 178. <https://doi.org/10.1186/1471-2148-12-178>
- Jakobsson, M., & Rosenberg, N. A. (2007). CLUMPP: A cluster matching and permutation program for dealing with label switching and multimodality in analysis of population structure. *Bioinformatics*, 23(14), 1801–1806. <https://doi.org/10.1093/bioinformatics/btm233>
- Janes, J. K., Miller, J. M., Dupuis, J. R., Malenfant, R. M., Gorrell, J. C., Cullingham, C. I., & Andrew, R. L. (2017). The K=2 conundrum. *Molecular Ecology*, 26(14), 3594–3602. <https://doi.org/10.1111/mec.14187>
- Jombart, T. (2008). ADEGENET: A R package for the multivariate analysis of genetic markers. *Bioinformatics*, 24(11), 1403–1405. <https://doi.org/10.1093/bioinformatics/btn129>
- Kearney, M., & Porter, W. (2009). Mechanistic niche modelling: combining physiological and spatial data to predict species' ranges. *Ecology Letters*, 12(4), 334–350. <https://doi.org/10.1111/j.1461-0248.2008.01277.x>
- Keightley, P. D., Ness, R. W., Halligan, D. L., & Hadrill, P. R. (2014). Estimation of the spontaneous mutation rate per nucleotide site in a *Drosophila melanogaster* full-sib family. *Genetics*, 196(1), 313–320. <https://doi.org/10.1534/genetics.113.158758>
- Keightley, P. D., Pinharanda, A., Ness, R. W., Simpson, F., Dasmahapatra, K. K., Mallet, J., Davey, J. W., & Jiggins, C. D. (2015). Estimation of the spontaneous mutation rate in *Heliconius melpomene*. *Molecular Biology and Evolution*, 32(1), 239–243. <https://doi.org/10.1093/molbev/msu302>
- Keller, I., Veltso, P., & Nichols, R. A. (2008). The frequency of rDNA variants within individuals provides evidence of population history and gene flow across a grasshopper hybrid zone. *Evolution*, 62(4), 833–844. <https://doi.org/10.1111/j.1558-5646.2008.00320.x>
- Kirschel, A. N. G., Nwankwo, E. C., Pierce, D. K., Lukhele, S. M., Moysi, M., Ogolowa, B. O., Hayes, S. C., Monadjem, A., & Brelsford, A. (2020). CYP2J19 mediates carotenoid colour introgression across a natural avian hybrid zone. *Molecular Ecology*, 29(24), 4970–4984. <https://doi.org/10.1111/mec.15691>
- Klicka, J., & Zink, R. M. (1997). The importance of recent ice ages in speciation: A failed paradigm. *Science*, 277(5332), 1666–1669. <https://doi.org/10.1126/science.277.5332.1666>
- Knowles, L. L. (2001). Genealogical portraits of speciation in montane grasshoppers (genus *Melanoplus*) from the sky islands of the Rocky Mountains. *Proceedings of the Royal Society B-Biological Sciences*, 268(1464), 319–324. <https://doi.org/10.1098/rspb.2000.1364>
- Knowles, L. L. (2009). Statistical phylogeography. *Annual Review of Ecology Evolution and Systematics*, 40, 593–612. <https://doi.org/10.1146/annurev.ecolsys.38.091206.095702>
- Knowles, L. L., & Carstens, B. C. (2007). Estimating a geographically explicit model of population divergence. *Evolution*, 61(3), 477–493. <https://doi.org/10.1111/j.1558-5646.2007.00043.x>
- Knowles, L. L., & Massatti, R. (2017). Distributional shifts – not geographical isolation – As a probable driver of montane species divergence. *Ecography*, 40(12), 1475–1485. <https://doi.org/10.1111/ecog.02893>

- Kutschera, V. E., Bidon, T., Hailer, F., Rodi, J. L., Fain, S. R., & Janke, A. (2014). Bears in a forest of gene trees: Phylogenetic inference is complicated by incomplete lineage sorting and gene flow. *Molecular Biology and Evolution*, 31(8), 2004–2017. <https://doi.org/10.1093/molbev/msu186>
- Lemonnier-Darcemont, M., & Darcemont, C. (2014). New observation of *Podisma pedestris* (Linne, 1758) forma macroptera (Orthoptera, Acrididae), in the Republic of Macedonia. *Articulata*, 29(1–2), 1–7.
- Liu, C. R., Berry, P. M., Dawson, T. P., & Pearson, R. G. (2005). Selecting thresholds of occurrence in the prediction of species distributions. *Ecography*, 28(3), 385–393. <https://doi.org/10.1111/j.0906-7590.2005.03957.x>
- Liu, X. M., & Fu, Y. X. (2015). Exploring population size changes using SNP frequency spectra. *Nature Genetics*, 47(5), 555–559. <https://doi.org/10.1038/ng.3254>
- Liu, X. M., & Fu, Y. X. (2020). Stairway Plot 2: demographic history inference with folded SNP frequency spectra. *Genome Biology*, 21(1), <https://doi.org/10.1186/s13059-020-02196-9>
- Maddison, W. P., & Knowles, L. L. (2006). Inferring phylogeny despite incomplete lineage sorting. *Systematic Biology*, 55(1), 21–30. <https://doi.org/10.1080/10635150500354928>
- Maier, P. A., Vandergast, A. G., Ostojia, S. M., Aguilar, A., & Bohonak, A. J. (2019). Pleistocene glacial cycles drove lineage diversification and fusion in the Yosemite toad (*Anaxyrus canorus*). *Evolution*, 73(12), 2476–2496. <https://doi.org/10.1111/evo.13868>
- Mallet, J., Besansky, N., & Hahn, M. W. (2016). How reticulated are species? *BioEssays*, 38(2), 140–149. <https://doi.org/10.1002/bies.201500149>
- Manichaikul, A., Mychaleckyj, J. C., Rich, S. S., Daly, K., Sale, M., & Chen, W. M. (2010). Robust relationship inference in genome-wide association studies. *Bioinformatics*, 26(22), 2867–2873. <https://doi.org/10.1093/bioinformatics/btq559>
- Marquez, E. J., & Knowles, L. L. (2007). Correlated evolution of multivariate traits: Detecting co-divergence across multiple dimensions. *Journal of Evolutionary Biology*, 20(6), 2334–2348. <https://doi.org/10.1111/j.1420-9101.2007.01415.x>
- Mason, P. L., Nichols, R. A., & Hewitt, G. M. (1995). Philopatry in the alpine grasshopper *Podisma pedestris* - A novel experimental and analytical method. *Ecological Entomology*, 20(2), 137–145. <https://doi.org/10.1111/j.1365-2311.1995.tb00439.x>
- McBreen, K., & Lockhart, P. J. (2006). Reconstructing reticulate evolutionary histories of plants. *Trends in Plant Science*, 11(8), 398–404. <https://doi.org/10.1016/j.tplants.2006.06.004>
- Melo-Ferreira, J., Boursot, P., Suchentrunk, F., Ferrand, N., & Alves, P. C. (2005). Invasion from the cold past: extensive introgression of mountain hare (*Lepus timidus*) mitochondrial DNA into three other hare species in northern Iberia. *Molecular Ecology*, 14(8), 2459–2464. <https://doi.org/10.1111/j.1365-294X.2005.02599.x>
- Morales-Agacino, E. (1951). Breves notas sobre los *Podismini* de la península ibérica (Orth. Acrid.). *EOS, Tomo Extraordinario*, 367–384.
- Muscarella, R., Galante, P. J., Soley-Guardia, M., Boria, R. A., Kass, J. M., Uriarte, M., & Anderson, R. P. (2014). *ENMeval*: An R package for conducting spatially independent evaluations and estimating optimal model complexity for MAXENT ecological niche models. *Methods in Ecology and Evolution*, 5(11), 1198–1205. <https://doi.org/10.1111/2041-210x.12261>
- Nevado, B., Contreras-Ortiz, N., Hughes, C., & Filatov, D. A. (2018). Pleistocene glacial cycles drive isolation, gene flow and speciation in the high-elevation Andes. *New Phytologist*, 219(2), 779–793. <https://doi.org/10.1111/nph.15243>
- Noguerales, V., Cordero, P. J., & Ortego, J. (2018). Integrating genomic and phenotypic data to evaluate alternative phylogenetic and species delimitation hypotheses in a recent evolutionary radiation of grasshoppers. *Molecular Ecology*, 27(5), 1229–1244. <https://doi.org/10.1111/mec.14504>
- Noguerales, V., García-Navas, V., Cordero, P. J., & Ortego, J. (2016). The role of environment and core-margin effects on range-wide phenotypic variation in a montane grasshopper. *Journal of Evolutionary Biology*, 29(11), 2129–2142. <https://doi.org/10.1111/jeb.12915>
- Nylander, J. A. A., Olsson, U., Alström, P., & Sanmartín, I. (2008). Accounting for phylogenetic uncertainty in biogeography: A Bayesian approach to dispersal-vicariance analysis of the thrushes (Aves: *Turdus*). *Systematic Biology*, 57(2), 257–268. <https://doi.org/10.1080/10635150802044003>
- Ortego, J., García-Navas, V., Noguerales, V., & Cordero, P. J. (2015). Discordant patterns of genetic and phenotypic differentiation in five grasshopper species codistributed across a microreserve network. *Molecular Ecology*, 24(23), 5796–5812. <https://doi.org/10.1111/mec.13426>
- Ortego, J., Gugger, P. F., & Sork, V. L. (2018). Genomic data reveal cryptic lineage diversification and introgression in Californian golden cup oaks (section *Protobalanus*). *New Phytologist*, 218(2), 804–818. <https://doi.org/10.1111/nph.14951>
- Ortego, J., Gutiérrez-Rodríguez, J., & Noguerales, V. (2021). Demographic consequences of dispersal-related trait shift in two recently diverged taxa of montane grasshoppers. *Evolution*, 75(8), 1998–2013. <https://doi.org/10.1111/evo.14205>
- Ortego, J., & Knowles, L. L. (2020). Incorporating interspecific interactions into phylogeographic models: A case study with Californian oaks. *Molecular Ecology*, 29(23), 4510–4524. <https://doi.org/10.1111/mec.15548>
- Papadopoulou, A., & Knowles, L. L. (2015a). Genomic tests of the species-pump hypothesis: Recent island connectivity cycles drive population divergence but not speciation in Caribbean crickets across the Virgin Islands. *Evolution*, 69(6), 1501–1517. <https://doi.org/10.1111/evo.12667>
- Papadopoulou, A., & Knowles, L. L. (2015b). Species-specific responses to island connectivity cycles: Refined models for testing phylogeographic concordance across a Mediterranean Pleistocene Aggregate Island Complex. *Molecular Ecology*, 24(16), 4252–4268. <https://doi.org/10.1111/mec.13305>
- Papadopoulou, A., & Knowles, L. L. (2016). Toward a paradigm shift in comparative phylogeography driven by trait-based hypotheses. *Proceedings of the National Academy of Sciences of the United States of America*, 113(29), 8018–8024. <https://doi.org/10.1073/pnas.1601069113>
- Papes, M., & Gaubert, P. (2007). Modelling ecological niches from low numbers of occurrences: Assessment of the conservation status of poorly known viverrids (Mammalia, Carnivora) across two continents. *Diversity and Distributions*, 13(6), 890–902. <https://doi.org/10.1111/j.1472-4642.2007.00392.x>
- Payseur, B. A., & Rieseberg, L. H. (2016). A genomic perspective on hybridization and speciation. *Molecular Ecology*, 25(11), 2337–2360. <https://doi.org/10.1111/mec.13557>
- Peterson, B. K., Weber, J. N., Kay, E. H., Fisher, H. S., & Hoekstra, H. E. (2012). Double digest RADseq: An inexpensive method for *de novo* SNP discovery and genotyping in model and non-model species. *PLoS One*, 7(5), e37135. <https://doi.org/10.1371/journal.pone.0037135>
- Petit, R. J., Aguinalde, I., de Beaulieu, J. L., Bittkau, C., Brewer, S., Cheddadi, R., Ennos, R., Fineschi, S., Grivet, D., Lascoux, M., Mohanty, A., Muller-Starck, G. M., Demesure-Musch, B., Palme, A., Martin, J. P., Rendell, S., & Vendramin, G. G. (2003). Glacial refugia: Hotspots but not melting pots of genetic diversity. *Science*, 300(5625), 1563–1565.
- Pfennig, K. S. (2016). Reinforcement as an initiator of population divergence and speciation. *Current Zoology*, 62(2), 145–154. <https://doi.org/10.1093/cz/zow033>
- Phillips, S. J., Anderson, R. P., & Schapire, R. E. (2006). Maximum entropy modeling of species geographic distributions. *Ecological*

- Modelling*, 190(3–4), 231–259. <https://doi.org/10.1016/j.ecolmodel.2005.03.026>
- Phillips, S. J., & Dudík, M. (2008). Modeling of species distributions with MAXENT: New extensions and a comprehensive evaluation. *Ecography*, 31(2), 161–175. <https://doi.org/10.1111/j.0906-7590.2008.5203.x>
- Pickrell, J. K., & Pritchard, J. K. (2012). Inference of population splits and mixtures from genome-wide allele frequency data. *PLoS Genetics*, 8(11), e1002967. <https://doi.org/10.1371/journal.pgen.1002967>
- Presá, J. J., García, M., Clemente, M., Barranco Vega, P., Correas, J., Ferreira, S., Hochkirch, A., Lemos, P., Odé, B., & Prunier, F. (2016a). *Podisma carpetana*: The IUCN Red List of Threatened Species 2016 (Publication no. e.T16084405A75089074). <https://doi.org/10.2305/IUCN.UK.2016-3.RLTS.T16084405A75089074.en>. <https://www.iucnredlist.org/species/16084405/75089074>
- Presá, J. J., García, M., Clemente, M., Barranco Vega, P., Correas, J., Ferreira, S., Hochkirch, A., Lemos, P., Odé, B., & Prunier, F. (2016b). *Podisma cantabricae*: The IUCN Red List of Threatened Species 2016 (Publication no. e.T16084528A75089065). <https://doi.org/10.2305/IUCN.UK.2016-3.RLTS.T16084528A75089065.en>. <https://www.iucnredlist.org/species/16084528/75089065>
- Pritchard, J. K., Stephens, M., & Donnelly, P. (2000). Inference of population structure using multilocus genotype data. *Genetics*, 155(2), 945–959. <https://doi.org/10.1093/genetics/155.2.945>
- R Core Team (2021). R: A language and environment for statistical computing. R Foundation for Statistical Computing. <https://www.R-project.org/>
- Rangel, T. F., Colwell, R. K., Graves, G. R., Fucikova, K., Rahbek, C., & Diniz, J. A. F. (2015). Phylogenetic uncertainty revisited: Implications for ecological analyses. *Evolution*, 69(5), 1301–1312. <https://doi.org/10.1111/evo.12644>
- Rosenberg, N. A. (2004). DISTRICT: A program for the graphical display of population structure. *Molecular Ecology Notes*, 4(1), 137–138. <https://doi.org/10.1046/j.1471-8286.2003.00566.x>
- Rosindell, J., Cornell, S. J., Hubbell, S. P., & Etienne, R. S. (2010). Protracted speciation revitalizes the neutral theory of biodiversity. *Ecology Letters*, 13(6), 716–727. <https://doi.org/10.1111/j.1461-0248.2010.01463.x>
- Schoville, S. D., Roderick, G. K., & Kavanaugh, D. H. (2012). Testing the 'Pleistocene species pump' in alpine habitats: lineage diversification of flightless ground beetles (Coleoptera: Carabidae: Nebria) in relation to altitudinal zonation. *Biological Journal of the Linnean Society*, 107(1), 95–111. <https://doi.org/10.1111/j.1095-8312.2012.01911.x>
- Schrago, C. G., & Seuanez, H. N. (2019). Large ancestral effective population size explains the difficult phylogenetic placement of owl monkeys. *American Journal of Primatology*, 81(3), e22955. <https://doi.org/10.1002/ajp.22955>
- Servedio, M. R., & Noor, M. A. F. (2003). The role of reinforcement in speciation: Theory and data. *Annual Review of Ecology and Systematics*, 34, 339–364. <https://doi.org/10.1146/annurev.ecolsys.34.011802.132412>
- Shcheglovitova, M., & Anderson, R. P. (2013). Estimating optimal complexity for ecological niche models: A jackknife approach for species with small sample sizes. *Ecological Modelling*, 269, 9–17. <https://doi.org/10.1016/j.ecolmodel.2013.08.011>
- Simmons, A. D., & Thomas, C. D. (2004). Changes in dispersal during species' range expansions. *American Naturalist*, 164(3), 378–395. <https://doi.org/10.1086/423430>
- Solís-Lemus, C., Bastide, P., & Ané, C. (2017). PHYLONETWORKS: A package for phylogenetic networks. *Molecular Biology and Evolution*, 34(12), 3292–3298. <https://doi.org/10.1093/molbev/msx235>
- Stamatakis, A. (2014). RAXML version 8: a tool for phylogenetic analysis and post-analysis of large phylogenies. *Bioinformatics*, 30(9), 1312–1313. <https://doi.org/10.1093/bioinformatics/btu033>
- Stewart, J. R., Lister, A. M., Barnes, I., & Dalen, L. (2010). Refugia revisited: individualistic responses of species in space and time. *Proceedings of the Royal Society B-Biological Sciences*, 277(1682), 661–671. <https://doi.org/10.1098/rspb.2009.1272>
- Sukumaran, J., & Knowles, L. L. (2017). Multispecies coalescent delimits its structure, not species. *Proceedings of the National Academy of Sciences of the United States of America*, 114(7), 1607–1612. <https://doi.org/10.1073/pnas.1607921114>
- Swofford, D. L. (2002). *paup**. *Phylogenetic analysis using parsimony (*and other methods)*. Version 4. Sinauer Associates.
- Takahashi, T., Nagata, N., & Sota, T. (2014). Application of RAD-based phylogenetics to complex relationships among variously related taxa in a species flock. *Molecular Phylogenetics and Evolution*, 80, 137–144. <https://doi.org/10.1016/j.ympev.2014.07.016>
- Tariel, J., Longo, G. C., & Bernardi, G. (2016). Tempo and mode of speciation in *Holacanthus* angelfishes based on RADseq markers. *Molecular Phylogenetics and Evolution*, 98, 84–88. <https://doi.org/10.1016/j.ympev.2016.01.010>
- Thom, G., Amaral, F. R. D., Hickerson, M. J., Aleixo, A., Araujo-Silva, L. E., Ribas, C. C., Choueri, E., & Miyaki, C. Y. (2018). Phenotypic and genetic structure support gene flow generating gene tree discordances in an Amazonian floodplain endemic species. *Systematic Biology*, 67(4), 700–718. <https://doi.org/10.1093/sysbio/syy004>
- Thomaz, A. T., & Knowles, L. L. (2020). Common barriers, but temporal dissonance: Genomic tests suggest ecological and paleo-landscape sieves structure a coastal riverine fish community. *Molecular Ecology*, 29(4), 783–796. <https://doi.org/10.1111/mec.15357>
- Thome, M. T. C., & Carstens, B. C. (2016). Phylogeographic model selection leads to insight into the evolutionary history of four-eyed frogs. *Proceedings of the National Academy of Sciences of the United States of America*, 113(29), 8010–8017. <https://doi.org/10.1073/pnas.1601064113>
- Tonzo, V., & Ortego, J. (2021). Glacial connectivity and current population fragmentation in sky islands explain the contemporary distribution of genomic variation in two narrow-endemic montane grasshoppers from a biodiversity hotspot. *Diversity and Distributions*, 27(9), 1619–1633. <https://doi.org/10.1111/ddi.13306>
- van Proosdij, A. S. J., Sosef, M. S. M., Wieringa, J. J., & Raes, N. (2016). Minimum required number of specimen records to develop accurate species distribution models. *Ecography*, 39(6), 542–552. <https://doi.org/10.1111/ecog.01509>
- Virdee, S. R., & Hewitt, G. M. (1994). Clines for hybrid dysfunction in a grasshopper hybrid zone. *Evolution*, 48(2), 392–407. <https://doi.org/10.2307/2410100>
- Wachter, G. A., Papadopoulou, A., Muster, C., Arthofer, W., Knowles, L. L., Steiner, F. M., & Schlick-Steiner, B. C. (2016). Glacial refugia, recolonization patterns and diversification forces in Alpine-endemic *Megabunus* harvestmen. *Molecular Ecology*, 25(12), 2904–2919. <https://doi.org/10.1111/mec.13634>
- Wallis, G. P., Waters, J. M., Upton, P., & Craw, D. (2016). Transverse alpine speciation driven by glaciation. *Trends in Ecology & Evolution*, 31(12), 916–926. <https://doi.org/10.1016/j.tree.2016.08.009>
- Wen, D. Q., Yu, Y., Hahn, M. W., & Nakhleh, L. (2016). Reticulate evolutionary history and extensive introgression in mosquito species revealed by phylogenetic network analysis. *Molecular Ecology*, 25(11), 2361–2372. <https://doi.org/10.1111/mec.13544>
- Wiens, J. A., Stralberg, D., Jongsomjit, D., Howell, C. A., & Snyder, M. A. (2009). Niches, models, and climate change: Assessing the assumptions and uncertainties. *Proceedings of the National Academy of Sciences of the United States of America*, 106, 19729–19736. <https://doi.org/10.1073/pnas.0901639106>
- Wisz, M. S., Hijmans, R. J., Li, J., Peterson, A. T., Graham, C. H., Guisan, A., & Distribut, N. P. S. (2008). Effects of sample size on the performance

of species distribution models. *Diversity and Distributions*, 14(5), 763–773. <https://doi.org/10.1111/j.1472-4642.2008.00482.x>

Zuna-Kratky, T., Fontana, P., Roesti, C., Braud, Y., Hochkirch, A., Monnerat, C., Rutschmann, F., & Presa, J. J. (2016). *Podisma pedestris*: The IUCN Red List of Threatened Species 2016 (Publication no. e.T16084622A70645980). <https://www.iucnredlist.org/species/16084622/70645980>

How to cite this article: Ortego, J., & Knowles, L. L. (2022). Geographical isolation versus dispersal: Relictual alpine grasshoppers support a model of interglacial diversification with limited hybridization. *Molecular Ecology*, 31, 296–312. <https://doi.org/10.1111/mec.16225>

SUPPORTING INFORMATION

Additional supporting information may be found in the online version of the article at the publisher's website.